

# Response Surface Optimization of Electro-Spun Polyvinyl Alcohol Nano-Fiber Membrane Process Parameters and its Characterization

Kibrom Alebel Gebru and Chandan Das\*

*Department of Chemical Engineering, Indian Institute of Technology Guwahati-781039, Assam, India*

**Abstract:** An empirical exploration into the effects of time duration, voltage supply, concentration and flow rate on the membrane average fiber diameter and surface pore size distribution were done using response surface methodology (RSM) based on central composite design (CCD). The average fiber diameter and average surface pore diameter of the membrane (i.e. 110 nm and 130 nm, respectively) were obtained at optimum input parameters of 45 min, 10 wt. %, 12 kV and 1.0 mL/h for time duration, concentration, voltage supply, and flow rate, respectively. The optimization study shows that the predicted versus actual values of both membrane fiber diameter and surface pore diameter are at  $R^2 = 0.96$ . In addition, the effect of glutaraldehyde on membrane crosslinking was also assessed for further studies. The results from FESEM images of the fabricated PVA nanofiber membranes using the optimized parameters revealed that the membranes showed smooth morphological structures without formation of beads. The thermo gravimetric analysis (TGA) results displayed an improvement in thermal stability after membrane crosslinking. From this study we have observed that the membrane average fiber diameter and surface pore diameter can be controlled by varying the electro-spinning parameters and can be utilized for wastewater treatment application.

**Keywords:** Electro-spinning, RSM, Crosslinking, PVA, Thermal analysis.

## 1. INTRODUCTION

During electro-spinning process, a high voltage (i.e. approximately 10 to 50 kV) is supplied in a polymer solution to the extent that charges are produced within the polymer solution. Once a sufficient amount of charge is supplied, a solution jet escapes from the needle-tip droplet causing in the development of the so called Taylor cone. After that, the electro-spinning jet travels to the grounded collector (i.e. with lower potential). The morphological structure of the electro-spun fibres can be influenced by processing parameters. Several polymer types can be electro-spun into nanofiber, providing that the molecular weight of polymers is sufficient and the solvent can be vaporized timely throughout the jet journey time over the given distance between the needle-tip and ground collecting plate. It is mentioned in the literature that more than hundred polymers, including polyvinyl alcohol have been effectively electrospun into nanofibers commonly from a polymer solution [1, 2]. The nanofiber jet can be condensed into a mat which forms a highly porous membrane structure. It is evident that the electrospun polymeric membrane possesses specific properties, including high specific surface area, high porosity and continuous interconnected fibers. On the other hand, they can be easily modified to have very good physical and chemical properties by blending polymer-inorganic

nano composites prior to electro-spinning and can be utilized for water and air filtration, tissue engineering, sensors, and other applications [3-5]. Therefore, as observed from the literature still further investigations are required to advance the electro-spinning process, specifically to fabricate membranes for the purpose of water treatments. Electro-spun nanofibrous membranes, such as; PVA/Chitosan, polyvinyl alcohol, and PVA/cyanobacterial extracellular polymeric materials composite membranes were fabricated for prospective water filtration applications using a microfiltration poly vinylidene fluoride as support membrane [6]. Electro-spun nanofibrous membranes with a conventional non-woven microfibrous support showing higher flux microfiltration were also reported. The polyvinyl alcohol nanofibrous non-woven membranes were directly fabricated on top of the porous support by using electro-spinning technique [7]. Another study presented a nanofiber thin film composite membrane crosslinked electro-spun polyvinyl alcohol nanofiber and was uniquely found to be a very effective support layer, specifically for forward osmosis applications, due to its very low tortuosity, very high porosity, and remarkable hydrophilic property [8]. It is known that PVA among synthetic polymers is easily soluble in water, non-toxic, relatively low-cost, stable in chemical and thermal conditions, and less degradable in most physiological environments. It is apparent that the polymer solution properties have the major impact in the electro-spinning process and the resulting membrane morphological structures. On the other hand, the

\*Address correspondence to this author at the Department of Chemical Engineering, Indian Institute of Technology Guwahati-781039, Assam, India; Tel: +91 361 2582268; Fax: +91 361 2582291; E-mail: cdas@iitg.ac.in

surface tension, viscosity, and electrical properties of the polymer solution play important role in the degree of elongation of the solution and in the development of beads along the fiber length [9]. Koski *et al.* [1] have studied the effects of polymer average molecular weight on the fibre structure of electro-spun polyvinyl alcohol (PVA). They have reported an average fibre diameter between 250 nm and 2  $\mu\text{m}$  and the fibre diameter increases with MW and concentration. From their experimental results, they have confirmed that at lower MW and/or concentrations, the fibres exhibit a circular cross-section. They have also observed flat fibres at high MW and concentrations. Furthermore, the effect of viscosity on the membrane morphology has also studied by Mohammad Ali Zadeh *et al.* [2]. According to their study, viscosity of the spinning solutions had played an important role on the morphology of the mullite nanofibres. Continuous electro-spun nanofibers with common cylindrical morphology were obtained when PVA content was 6 wt. %. Further increasing the amount of PVA in the pre spinning solution led to excessively high viscosity level, making the shape of the resulting mullite nanofibers wide and flat ribbon. Other important parameters that influence the electro-spinning process are voltage supply, feed rate, solution temperature, collector type, needle diameter, and the collector-needle tip distance. Barhate *et al.* [10] have studied the effect of electro-spinning process parameters on structural and transport properties of the electro-spun membranes. They have mentioned that the pore size and fiber entanglements can be optimized to enhance the pore size distribution, porosity, pore inter-connectivity, and permeability performances of the electro-spun membranes. Finally, they have suggested that an optimized structure of the membrane can be achieved by coordinating the collection rates, and applied voltage. The shapes and the sizes of nanofiber membranes are controlled through numerous parameters, like, conductivity, concentration, viscosity, and surface tension of the polymeric solutions. Though all the parameters are significant factors, polymeric solution concentration and applied voltage have considered as the most significant on the final characteristics of electro-spun fibers. The polymeric solution properties had the main substantial effect in the electro-spinning processes. The viscosity of the solution, surface tension, and its conductivity also determined the degree of elongations of the polymeric solution, which possibly had an influence on the diameters of the resulting electro-spun fibres [9]. As observed from the above literatures, the effect of the

electro-spinning parameters on the final properties of the membrane was investigated conventionally. Therefore, it is crucial to scientifically examine the impact of different electro-spinning parameters on the response of experimental results using optimization technique.

In this study, electro-spun poly vinyl alcohol was prepared using electro-spinning technique and two parameters (i.e. membrane average fiber diameter and membrane surface pore diameter) were optimized using response surface methodology (RSM). Polymer concentration, voltage supply, time duration, and solution flow rate were optimized based on central composite design (CCD). An effort was also given to further investigate the effect of electro-spinning process time duration on the resulting membranes, which was introduced as a new field along with the above important electro-spinning parameters. On the other hand, this study also aims to realize the interaction between process parameters with the experimental responses (i.e. membrane average fiber diameter and membrane surface pore diameter). The experimental and predicted values (which were found from the mathematical model) were compared to validate the model and were able to predict the optimum independent parameters for the preparation of micro/ultra-filtration electro-spun PVA membranes. Therefore, the first objective of the present work was optimization of the electro-spinning parameters and fabrication of the membrane using selected electro-spinning time duration (25, 35, 45, and 60 min). Secondly, electro-spun PVA membrane was cross-linked using glutadaraldehyde to evaluate the effect of crosslinking. We believe that this work will have substantial contribution in the field of membrane preparation for the purpose of waste water treatment applications.

## 2. MATERIALS AND METHODS

### 2.1. Materials

Polyvinyl alcohol, MW. 80,000, 98-99 mole % hydrolyzed, was purchased from Loba Chemie Pvt. Ltd, India, acetone (99.9% purity), Glutaraldehyde (GA) (25% aqueous solution) and hydrochloric acid (35% aqueous solution) were purchased from Merck, India. First, the PVA solutions were prepared by dissolving the polymer in distilled water at 70  $^{\circ}\text{C}$  with continuous stirring overnight and subsequently cooled to room temperature ( $28\pm 2$   $^{\circ}\text{C}$ ) earlier to electro-spinning process.

## 2.2. Methods

Electro-spun PVA membranes were prepared by using electro-spinning technique. During electro-spinning process, a high voltage is supplied to a polymeric solution in the syringe pump such that, charges are induced within the polymer solution (Figure 1). When charges inside the solution become sufficiently high amount and able to overcome the surface tension of the solution droplet, a solution jet erupts from the needle-tip drop results in the development of the so called Taylor cone. Finally the jet travels to the rotating collector with state of lower potential. Electro-spinning was performed using a NABOND NEU (China) electro-spinning unit at room temperature. The polymer solution was loaded into a 50 mL syringe with a needle (inner diameter of 0.4 mm). According to the design of experiments summary (Table 1), a polymer solution varied from 6 to 19.5 wt. %, an electric field of 5 to 25 kV was applied throughout the process and the fluid feed rate was 1 to 3 mL/h and time duration between 25 to 77.5 min. All the prepared fibers were deposited on a rotating collector, where the gap between the needle-tip and the collecting plate was fixed at 100 mm. Using the optimized electro-spinning parameters (concentration, voltage supply, and feed rate), the PVA membranes were prepared for the selected time durations (i.e. 25, 35, 45 and 60 min) to further investigate the impact of deposition time on the surface pore diameters, fiber

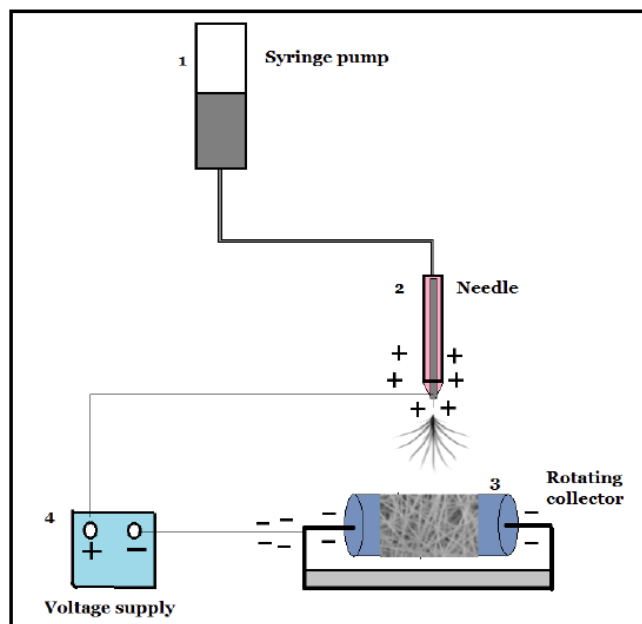


**Figure 1:** Schematic of the electro-spinning equipment, (1) syringe pump, (2) needle, (3) rotating collector and (4) voltage supply.

diameter, surface areas, porosity, and morphological structures of the electro-spun membranes. Surface tension, viscosity, and conductivities of the solutions were determined using a tensiometer (Kruss tensiometer K<sub>9</sub>), Viscometer (Anton Paar, Physica MCR 30, Austria) and a conductivity meter (ELICO, India), respectively.

## 2.3. Response Surface Methodology using Design of Expert

Design of experiment (DOE) has been known as an appropriate optimization tool in order to investigate and optimize the impact of electro-spinning parameters [11, 12]. The DOE technique is employed to reduce the number of experiments to be performed. Moreover, one of the effective optimization techniques in order to obtain the optimal conditions in a multi-variable scheme is response surface methodology (RSM) [13, 14]. Recently, the RSM optimization technique has been effectively employed in numerous processes to attain the optimal conditions. Furthermore, the central composite design (CCD) is a suitable experimental design technique among various approaches, which provides high quality estimates in studying interaction, quadratic, and linear effects of parameters [15]. Therefore, the optimization of the above parameters for polyvinyl alcohol based solutions was the preliminary point of this work. The theory and definition of some terms regarding RSM optimization process has been explained in detail by Bezerra *et al.* [13], Yordem *et al.* [12], and Ahmadipourroudposht *et al.* [16]. Our design plan including four input factors (i.e. time duration (min), voltage supply (kV), polymer concentration (wt. %), and feed rate (mL/h) and responses (R<sub>1</sub> and R<sub>2</sub> i.e. membrane fiber diameter and membrane surface pore diameter, respectively) for each experiment is presented in Table 1. These four input factors have been selected for designing purpose and their results were chosen based on preliminary investigation. The input factors are varied over five levels: high value (+1), the center point (0), low level (-1) and two outer points (- $\alpha$  and + $\alpha$  value), and the details are outlined in Table S1 in the Supporting Information. CCD comprises of design points and axial points that consisting of a total of 30 experimental run are used to examine the experimental data. These data are finally used to optimize the electro-spinning process parameters. The output variables (i.e. membrane fiber diameter and membrane surface pore diameter) are measured from the selected mathematical model with significant terms and the model was not aliased.

**Table 1: Design of Experiments Summary and Experimental Responses for Central Composite Design (CCD)**

Run	Factor1, A: Time duration (min)	Factor 2, B:Voltage supply (kV)	Factor 3, C: Concentration (Wt. %)	Factor 4, D:Flow rate (mL/h)	Response 1, Fiber diameter (nm)	Response 2, Surface pore diameter (nm)
1	42.5	15.0	10.5	4.0	179	155
2	25.0	20.0	6.0	3.0	95	90
3	42.5	15.0	10.5	2.0	105	109
4	25.0	10.0	15.0	1.0	117	180
5	25.0	10.0	6.0	1.0	106	144
6	7.5	15.0	10.5	2.0	129	267
7	60.0	10.0	15.0	1.0	125	207
8	60.0	20.0	6.0	1.0	76	132
9	42.5	15.0	10.5	2.0	100	107
10	42.5	15.0	10.5	2.0	103	111
11	60.0	10.0	15.0	3.0	78	192
12	25.0	20.0	15.0	1.0	50	193
13	42.5	15.0	1.5	2.0	46	90
14	60.0	10.0	6.0	1.0	47	149
15	60.0	20.0	15.0	3.0	39	270
16	42.0	15.0	10.5	2.0	107	108
17	42.5	15.0	10.5	0.0	135	200
18	25.0	20.0	15.0	3.0	25	290
19	60.0	20.0	6.0	3.0	55	90
20	60.0	10.0	6.0	3.0	150	50
21	42.5	15.0	10.5	2.0	104	110
22	60.0	20.0	15.0	1.0	133	230
23	42.5	15.0	19.5	2.0	20	310
24	42.5	5.0	10.5	2.0	160	60
25	25.0	20.0	6.0	1.0	80	98
26	77.5	15.0	10.5	2.0	78	169
27	42.5	25.0	10.5	2.0	56	100
28	42.5	15.0	10.5	2.0	103	109
29	25.0	10.0	6.0	3.0	256	80
30	25.0	10.0	15.0	3.0	138	200

## 2.4. Characterization

Morphological analysis of electro-spun PVA nanofiber membrane was done using a high resolution field emission scanning electron microscopy (FESEM, ZEISS). The chemical structures of the electro-spun PVA membranes were characterized by means of Fourier transform infrared (FTIR) spectrophotometer (IR affinity-1, Shimadzu, Japan). All the spectrums were obtained in the FTIR transmittance mode by accumulations of 40 scans using  $4\text{ cm}^{-1}$  resolutions and a wave number from 500 to  $4000\text{ cm}^{-1}$  range. The thermal degradation analysis was conducted by Thermo-Microbalance (Thermo gravimetric Analyser

(TG 209 F1 Libra®, Germany). The TGA results were obtained in the range of 30 to  $800\text{ }^{\circ}\text{C}$  in nitrogen atmosphere using a gas flow rate of  $40\text{ mL/min}$  at a heating rate of  $10\text{ }^{\circ}\text{C/min}$ . The membrane sample was loaded into a platinum sample pan. The graphs were obtained by plotting weight (%) vs. temperatures ( $^{\circ}\text{C}$ ).

## 2.5. Cross-Linking of Electro-Spun PVA

The effect of crosslinking of electro-spun PVA nanofibers membranes was studied. The cross-linking procedure and optimization have been done following the procedure suggested by Wang *et al.*, 2006. Accordingly, electro-spun PVA samples were dipped in

a solution containing 0.01N hydrochloric acid and 30 mM of glutaraldehyde/acetone for about 1 day. The cross-linked PVA membranes were withdrawn and rinsed using distilled water several times and then dried out.

### 3. RESULTS AND DISCUSSIONS

#### 3.1. Statistical Analysis (ANOVA) and Response Surface of Electro-Spinning Parameters

The statistical analyses of the electro-spinning parameters were performed using design expert software. ANOVA test was employed in order to perform the statistical tests for significance of model, individual model terms and lack of fit. It is obvious that a significant model is needed and "Prob. > F" values less than 0.05 shows significance of the model and the individual model terms. The ANOVA results for both fiber diameter (FD) distribution and surface pore diameter (SPD) distribution were analyzed. In both cases the lack-of-fit test values were insignificant, which are desired as we need a model that fits.

##### 3.1.1. Membrane Fiber Diameter

The relationship between electro-spinning process factors (i.e. time duration, voltage supply, concentration, and flow rate) and the expected responses (i.e. membrane fiber diameter and membrane surface pore diameter) are plotted graphically after mathematical analysis of the experimental data. Figure 2 shows the three dimensional response surface for membrane fiber diameter. As already observed from these figures, the factors involved in the membrane electro-spinning process exhibited non-linear effects on the membrane fiber diameter. The highest membrane average fiber diameter (i.e. 256 nm) was obtained at 25 min, 10 kV, 15 wt. %, and 3 mL/h (run 29) of time duration, voltage supply, polymer concentration, and flow rate, respectively. On the other hand, the lowest membrane average fiber diameter (i.e. 20 nm) was obtained at 42.5 min, 15 kV, 19.5 wt. % and 2 mL/h (run 23). As clearly showed in the three dimensional plots (i.e. Figure 1a, b, c, d and e), the membrane fiber diameter exhibited a decreasing trend from 140.6 nm to 72.9 nm as the voltage supply raised from 10 kV to 20 kV, where the polymer concentrations and flow rates were kept at 10.5 wt. % and 2 mL/h, respectively. On the other hand, As observed from the experimental results, continuous fibrous structures were obtained for 6 wt. % PVA aqueous solution concentrations, where the fibers contained many twists, branches and were highly

interconnected. At higher concentrations, the cross-sections of the fibers were spherical, but once the concentration of the solution was increased above 19.5 wt. %, the fiber diameter and inter fiber spacing was increased and there was a slow change from circular to flat ribbon like structure of the fibers [1, 2]. On the other hand, when the PVA concentration was lowered below 6 wt. %, the formation of large beads and non-uniform entanglement of fibres was observed. This result is may be accredited to an increasing in the surface tension or decreasing concentration of the polymer solution [6]. At relatively high voltage supply (15 kV), as the polymer concentration was raised from 6 wt. % to 8.25 wt. %, the average fiber diameter of the membrane was increased from 72.9 nm to 114 nm. Further increasing of the concentration above 8.25 wt. %, the average fiber diameters seem to have slight difference. Even though, the average fiber diameter is expected to increase with increasing the polymer concentration, in this case the high voltage supply seems to control the spinning of fibers with large diameters. The analysis of variance and regression model for the four model terms are presented in Table S2 in the Supporting Information where, the model F-value of 22.63 implies the model is significant. There is only a 0.01% chance that a "Model F-Value" this large could occur due to noise. As observed from the results the model terms such as, A, B, C, D, AB, AC, AD, BD, CD, C<sup>2</sup>, D<sup>2</sup> are significant, where their Prob. > F" values are below 0.05. Moreover, the voltage supply seems to be highly significant factor when compared with the other significant input factors (time duration, concentration, and flow rate). The values greater than 0.10 indicate that the model terms are not significant. The "Lack of Fit F-value" of 1.07 implies the Lack of Fit is not significant relative to the pure error. There is a 50.12 % chance that a "Lack of Fit F-value" this large could occur due to noise. Non-significant lack of fit is good that we want the model to fit. The following equation is the final equation in terms of coded factors which is developed using central composite design to designate the curvatures around the optimal point.

$$\begin{aligned}
 FD = & 95 - 11.08(A) - 28(B) - 8.83(C) \\
 & + 7.92(D) + 16.88(A \times B) \\
 & + 15.88(A \times C) - 13.75(A \times D) + 2.63(B \times C) \\
 & - 22(B \times D) - 24.5(C \times D) \\
 & + 1.75(A^2) + 2.88(B^2) - 15.88(C^2) + 15.12(D^2)
 \end{aligned} \tag{1}$$

The reliability of regression models for membrane fiber diameter was described on the basis of high values of R<sup>2</sup> (0.96), which shows that this model is well

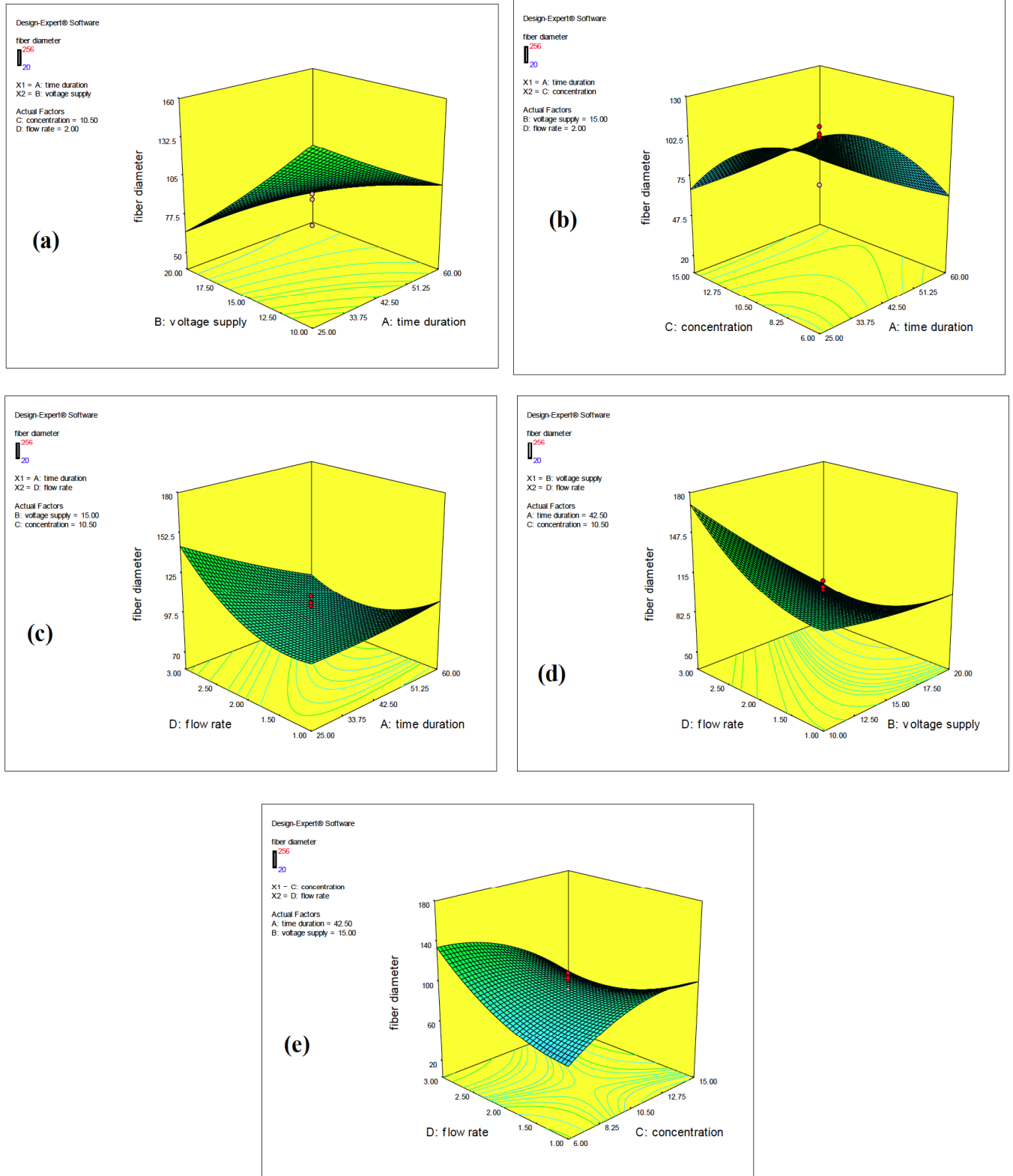


**Figure 2:** Three dimensional Response surface plot of (a) voltage supply and time duration, (b) concentration and time duration, (c) flow rate and time duration, (d) flow rate and voltage supply, and (e) flow rate and concentration for membrane fiber diameter.

fitted to the experimental values. On the other hand, the "Pred R-Squared" of 0.80 is in a reasonable agreement with the "Adj R-Squared" of 0.91. "Adeq

Precision" measures the signal to noise ratio and a ratio greater than 4 is desirable, where this model's ratio of 22.5 indicates an adequate signal.

### 3.1.2. Membrane Surface Pore Diameter

The three dimensional response surface plots, which show the impact of input factors (i.e. time duration, concentration, voltage supply, and flow rate) on membrane surface pore diameter, are presented in Figure 3. The maximum average membrane surface pore diameter of 310 nm was attained at a time duration of 42.5 min, voltage supply of 15 kV, concentration of 19.5 wt. % and flow rate of 2 mL/h (run 23) whereas the minimum average membrane surface pore diameter of 50 nm was achieved at a time duration of 60 min, voltage supply of 10 kV, concentration of 6 wt. % and flow rate of 3 mL/h (run 20). These results indicate that the concentration seems to have greater contribution on the variation in membrane surface pore diameter (Figure 3b and d). On the other hand, as shown from Figure 3a, the average surface pore diameter was decreased from 142 nm to 115 nm as the deposition time was increased from 25 to 51 min. These results can be explained due to the entanglement of fibers as the

electro-spinning time duration was increased. However, when the deposition time duration further increases beyond 51 min, the surface pore diameter showed a slightly increasing trend. At maximum polymer concentration of 19.5 wt. % (Run 23), it is observed that the surface pore diameter is high (310 nm), compared to the membranes prepared from less polymer concentration of (10.5) (Run 28), where the surface pore diameter was 100 nm. This incident is due to the increase in fiber diameter of the membrane, as the concentration of the solution was increased. The Model F-value of 27.15 implies the model is significant. There is only a 0.01% chance that a "Model F-Value" this large could occur due to noise. The values of "Prob > F" less than 0.05 indicate model terms are significant. In this case B, C, BC, BD, CD,  $A^2$ ,  $B^2$ ,  $C^2$ ,  $D^2$  are significant model terms. The values greater than 0.10 indicate the model terms are not significant. The "Lack of Fit F-value" of 4.35 implies there is a 5.92 % chance that a "Lack of Fit F-value" this large could occur due to noise. The following equation is the final equation in terms of coded factors which is developed using central

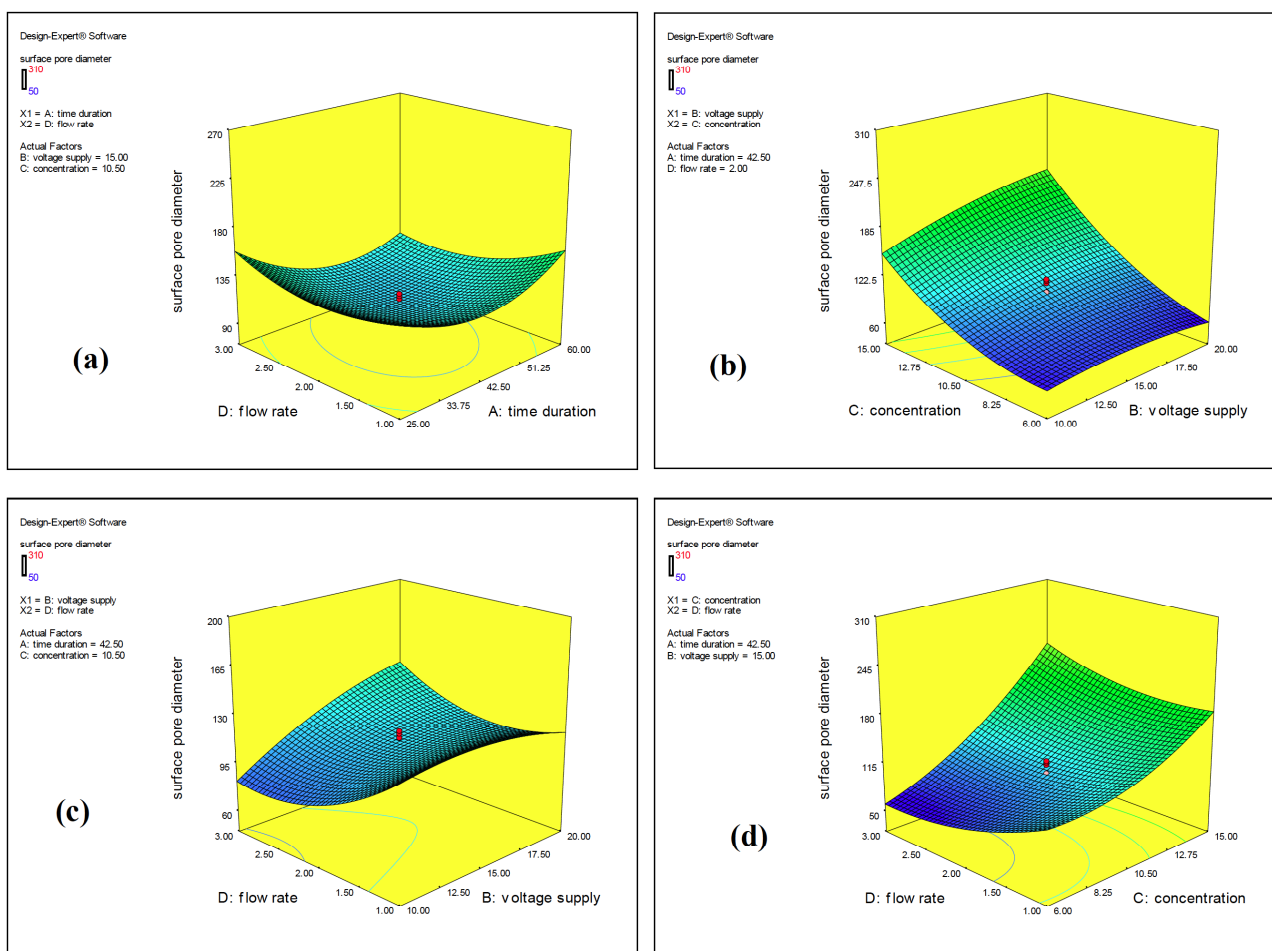


**Figure 3:** Three dimensional Response surface plot of (a) flow rate and time duration, (b) concentration and voltage supply, (c) flow rate and voltage supply, and (d) flow rate and concentration for membrane surface pore diameter.

composite design to designate the curvatures around the optimal point.

$$SPD = 107.33 + 11.29(B) + 57.4(C) - 10.06(A \times D) + 13.56(B \times C) + 15.31(B \times D) + 22.19(C \times D) + 26.55(A^2) - 7.95(B^2) + 22.05(C^2) + 16.43(D^2) \quad (2)$$

The reliability of regression models for membrane surface pore diameter was described on the basis of high values of  $R^2$  (0.96), which shows that this model is well fitted to the experimental values. On the other

hand, the "Pred R-Squared" of 0.80 is in a reasonable agreement with the "Adj R-Squared" of 0.93. "Adeq Precision" measures the signal to noise ratio. A ratio greater than 4 is desirable and the ratio of 19.7 in this model indicates an adequate signal.

### 3.2. Model Verification on the Basis of Statistical Analysis

The effects of the interactions among the input electro-spinning parameters were examined by using

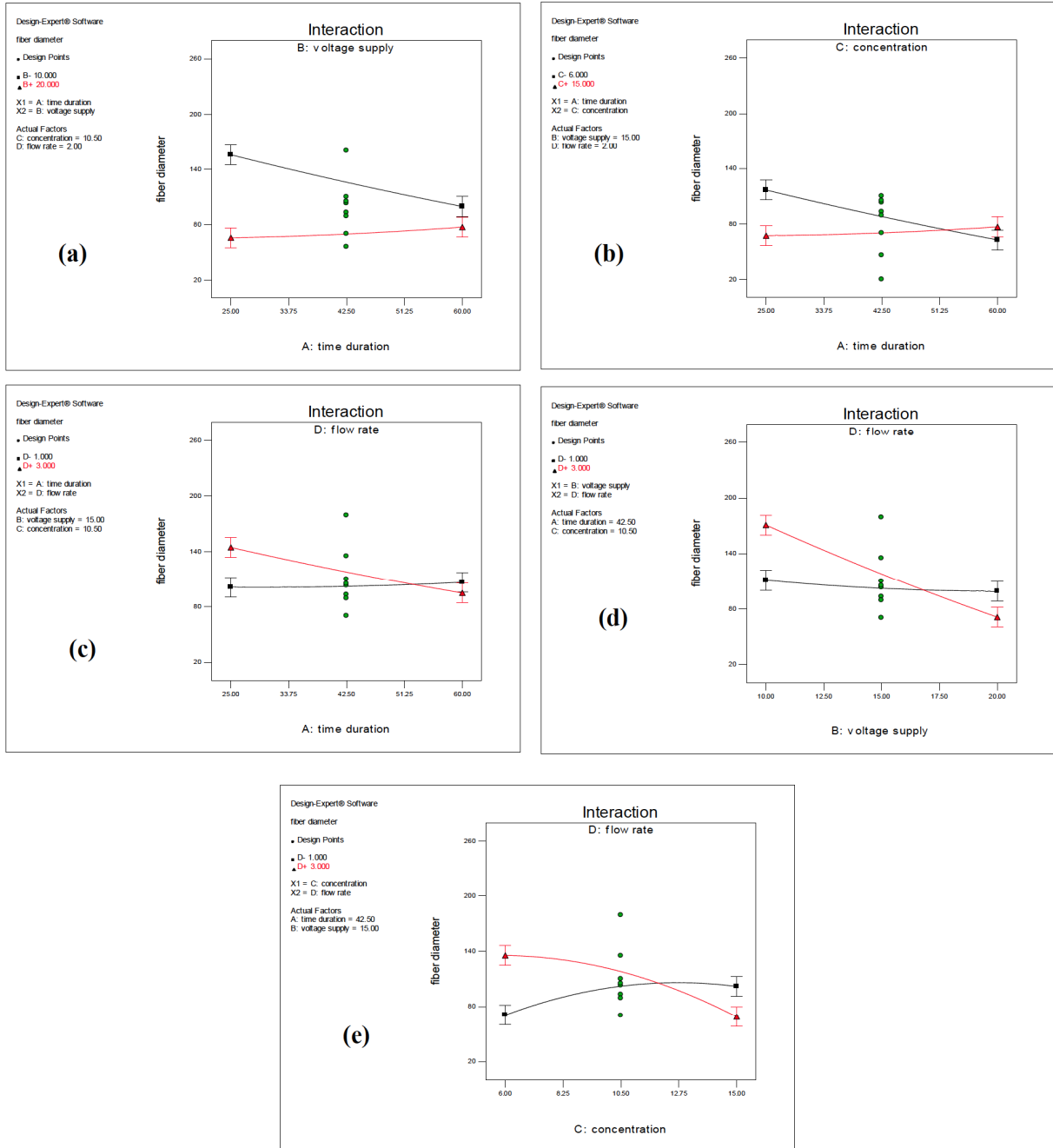


**Figure 4:** The interaction plots of (a) time duration and voltage supply; (b) time duration and concentration; (c) time duration and flow rate; (d) flow rate and voltage supply; and (e) flow rate and concentration for membrane fiber diameter.

RSM optimization technique. This optimization tool is useful in investigating the effect of binary combination of two input factors. The plots of the interaction between the input parameters are presented in Figures 4 and 5 for fiber diameters and surface pore diameter, respectively. As clearly observed from Figure 4, all the interaction plots exhibited non-parallel curvatures. From these results it is suggested a strong interaction between the variables (i.e. AB, AC, AD, BD, and CD) for membrane fiber diameters. As presented in Table S2 in the Supporting Information, BD and CD seemed to be highly significant model terms. Therefore, from this study it can be suggested that, the effect of voltage supply and concentration are highly significant input parameters for average fiber diameter of the membrane.

It is clearly seen from Figure 5 that the interactions of all the input factors (i.e. time duration, voltage supply, concentration, and flow rate) have significant effect on the surface pore diameter distribution. The interaction plots showed non-parallel curvatures and it is suggested that, there is a strong interaction between

the variables (i.e. AD, BC, BD, and CD) for membrane surface pore diameters. As shown in Table S2 in the Supporting Information, BD and CD seemed to be highly significant model terms when compared with the other model terms. In this case the most significant factors are voltage supply and concentration. On the other hand, the effects of the interactions of time duration and flow rate with the other parameters on the surface pore diameter of the electro-spun PVA membranes are investigated. This model suggested that the flow rate and time duration are more significant when they are in combination with other parameters than alone.

Figure 6 shows the actual versus predicted value plots where, the predicted values attained from regression model were compared with the experimental values to check the reliability and suitability of empirical model for individual responses. Therefore, the comparison between predicted and actual values for membrane fiber diameter and membrane surface pore diameter are presented in Figure 6a and d, respectively. As clearly shown from the figures, all the

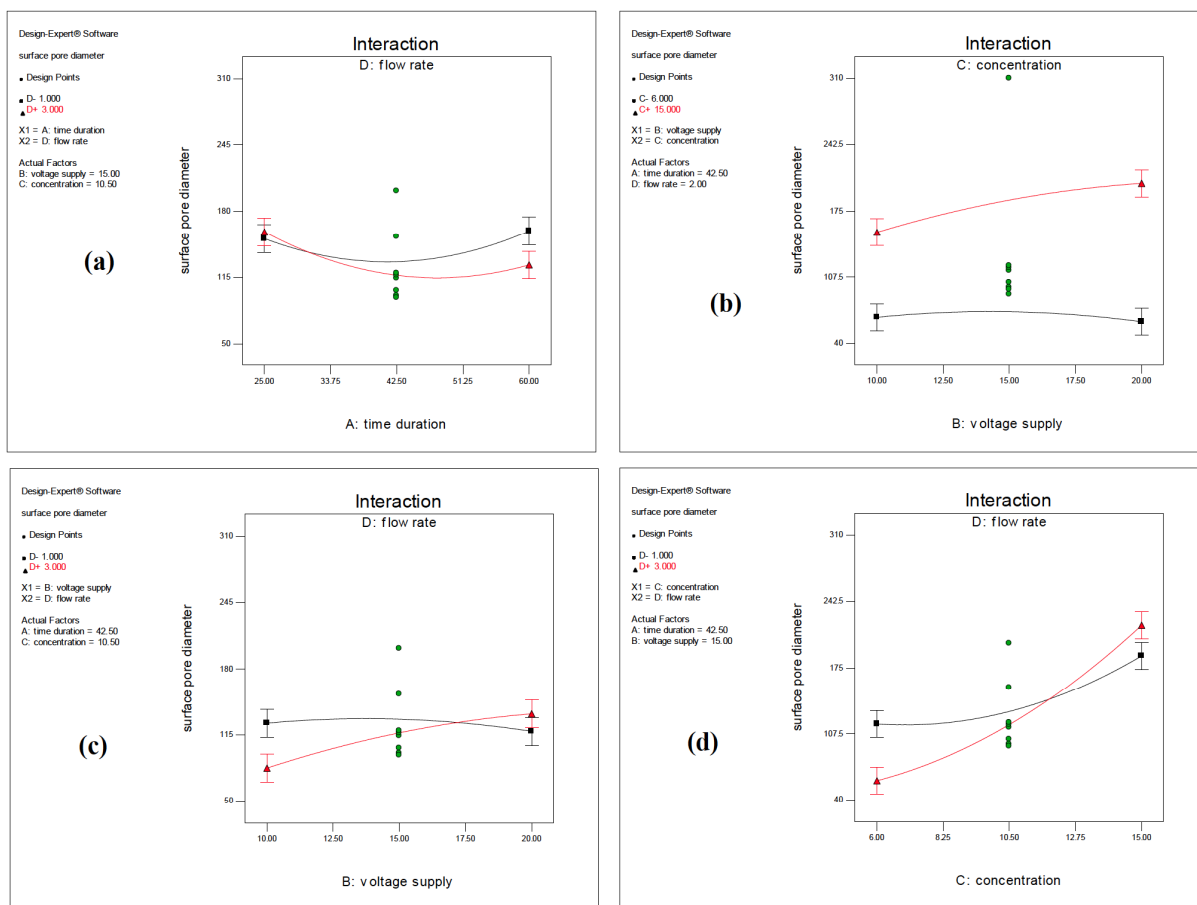


**Figure 5:** The interaction plots of (a) time duration and flow rate; (b) voltage supply and concentration; (c) voltage supply and flow rate; and (d) flow rate and concentration for membrane surface pore diameter.

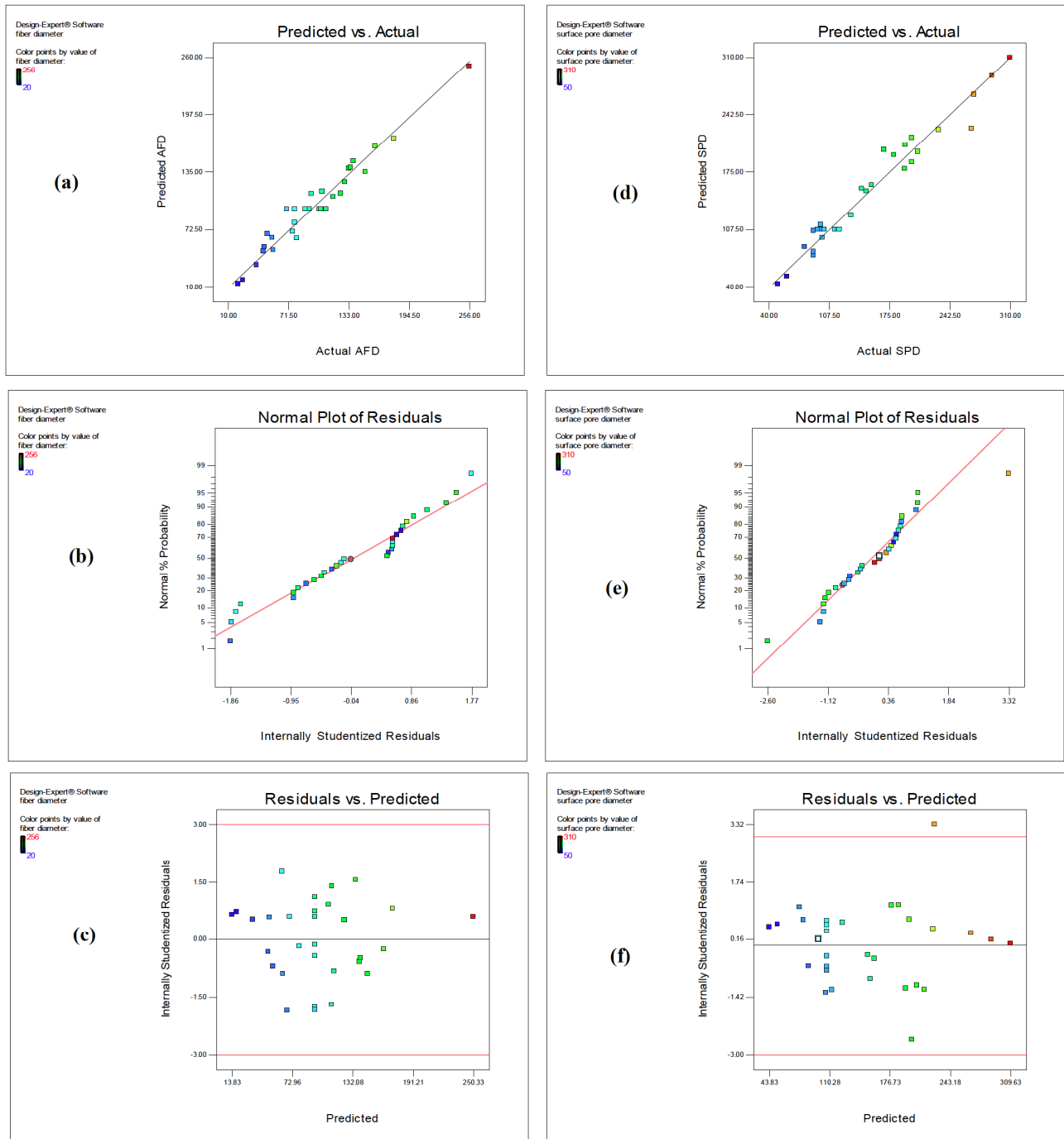


**Figure 6:** Plots of predicted versus actual values of membrane (a) fiber diameter ( $R^2 = 0.96$ ) and (d) surface pore diameter ( $R^2 = 0.96$ ); Normal probability plot of residual (b) membrane fiber diameter and (e) membrane surface pore diameter; Plot of residual vs. predicted of (c) membrane fiber diameter and (f) membrane surface pore diameter.

design points are distributed near the straight line, where the points above the straight line are over-estimated and below the straight line are under-estimated. Based on these results we can conclude that the estimated models are acceptable and there are no violations of constant variance assumptions. Furthermore, according to the data, the empirical model attained from CCD can be used as a predictor for the optimization of the four input parameters to

achieve a required average fiber diameter and surface pore diameter depending on the application interest. Figure 6b and e show the normal probability plot of residuals for fiber diameter and surface pore size, respectively. The plots in Figure 6b and e ensured that no abnormality signal of the experimental results was observed. Falling of the residual points on a straight line suggests that the errors are normally distributed. On the other hand, Figure 6c and f show the plots of

the residuals versus predicted responses for the membrane fiber diameter and membrane surface pore diameter, respectively. The random scattering of all experimental data points across the horizontal line of residuals suggests that the projected models are suitable.

### 3.3. Optimization Study

The investigation of the optimized input parameters (electro-spinning parameters) was done through a desirability function ( $D$ ) for two responses using eq. 3 [17]. The optimum time duration, concentration, voltage supply, and flow rate for preparation of the electro-spun membrane predicted from all responses with high or low limit of inputs can be satisfied with the desirability function ( $D$ ).

$$D = \left[ \prod_{i=1}^N d_i^{r_i} \right]^{1/\sum r_i} \quad (3)$$

Where  $D$  is the desirability function,  $N$  is the number of responses,  $r_i$  refers to the significance of a particular response, and  $d_i$  indicates the partial desirability function for specific responses. The desirability plot presented in Figure 7 confirms that the desirable time duration, concentration, voltage supply and flow rate are 43.48 min, 10.67 kV, 10.89 wt. %, and 1.01 mL/h, respectively, which gave optimized average fiber diameter of 110 nm and average surface pore diameter of 130 nm. The prediction of desirable input variables is also confirmed with the optimized input variables calculated from central composite design (listed in Table S3 in the Supporting Information). This

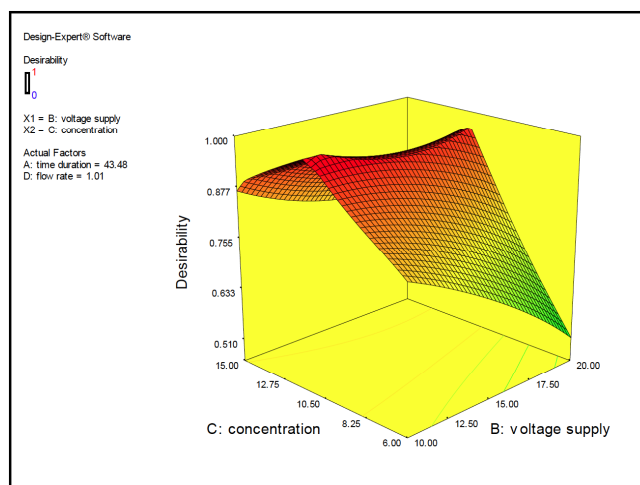


**Figure 7:** Response surface plot of desirability operating region: voltage supply and concentration of 10.67 kV and 10.89 wt. %, respectively.

optimization study shows that the desirability value of the model is  $D = 1.00$ .

This study draws the conclusions of an empirical exploration into the effects of time duration, voltage supply, concentration, and flow rate (while the distance and collector rotating speed were kept constant) on fiber diameter and surface pore size distribution during the preparation of electro-spun PVA membranes. Therefore, 10 wt. % aqueous PVA solutions were chosen as the optimized solution concentration; an applied voltage of 12 kV was selected throughout the process; and the feed rate was 1.0 mL/h by means of a 50 mL syringe using needle of 0.4 mm internal diameter. For further investigation on the effect of time duration, membranes were prepared at 25, 35, 45, and 60 min. The conductivity, surface tension, and viscosity values of the PVA solution were  $0.079 \text{ mS cm}^{-1}$ ,  $73.7 \text{ mN/m}$ ,  $0.299 \text{ Pa.s}$ , respectively.

### 3.4. Morphological Study (FESEM)

The FESEM images of the electro-spun PVA fibers obtained with 10 wt. % for different electro-spinning durations are presented in Figure 8. Fabricated PVA nanofiber membranes showed a smooth morphological structure, without developing beads. The fiber diameter distributions and surface pore diameters of the membranes were measured using image J software from FESEM images. More than 100 fibers of each membrane sample were measured using Image J software in order to get the average fiber diameter. As shown from Figure 8a<sub>2</sub>, b<sub>2</sub>, c<sub>2</sub>, d<sub>2</sub>, the fiber diameter results indicated those diameters between 78 and 276 nm for 25 min (a<sub>2</sub>); between 81 and 190 nm for 35 min (b<sub>2</sub>); between 59 and 160 for 45 min (c<sub>2</sub>) and between 37 and 199 nm for 60 min (d<sub>2</sub>). The average fiber diameters were varied as 124, 117, 100 and 88 nm for samples designated as M<sub>x</sub> (x=25, 35, 45, 60 min), respectively. It can be seen from the FESEM images presented in Figure 8a<sub>1</sub>, b<sub>1</sub>, c<sub>1</sub>, d<sub>1</sub> that the slight decrease in average fiber diameter can be related to increasing in ambient temperature during the electro-spinning duration. If the electro-spinning duration of the surrounding electric field delays, the surrounding temperature may increase due to increase in an electron temperature because of collision between the charges. Therefore, increasing temperature has the effect of decreasing the viscosities of the polymeric solutions, increasing solvent evaporation rate, and also may cause a high degree of polymer solubility within the solvent. As a result of these effects, the coulombic forces would be able to affect the surface tension of the

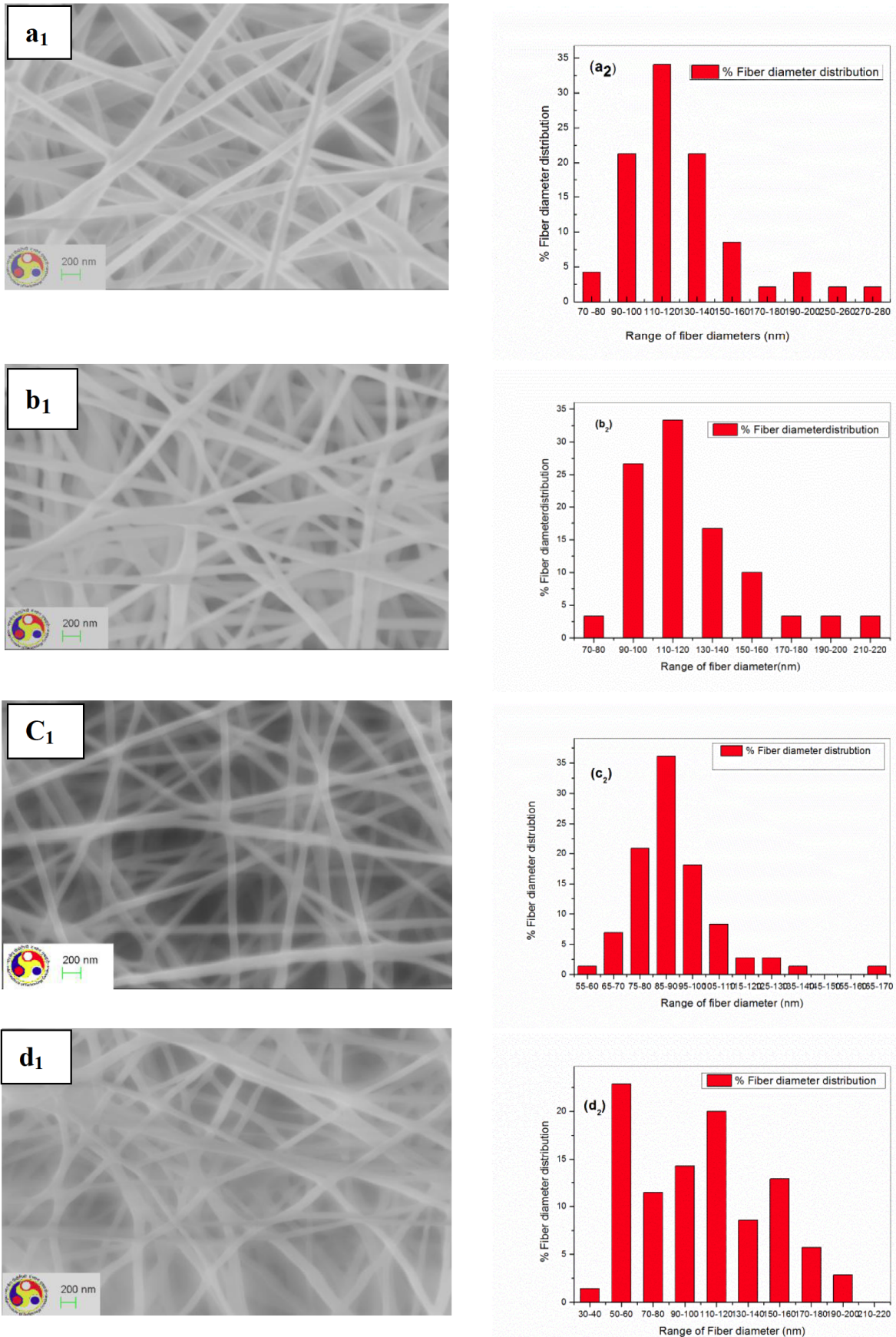


**Figure 8:** FESEM images of the ePVA fibres and their corresponding fibre diameter distribution at different process time, (**a<sub>1</sub>**, **a<sub>2</sub>**) 25 min, (**b<sub>1</sub>**, **b<sub>2</sub>**) 35 min, (**c<sub>1</sub>**, **c<sub>2</sub>**) 45 min and (**d<sub>1</sub>**, **d<sub>2</sub>**) 60 min.

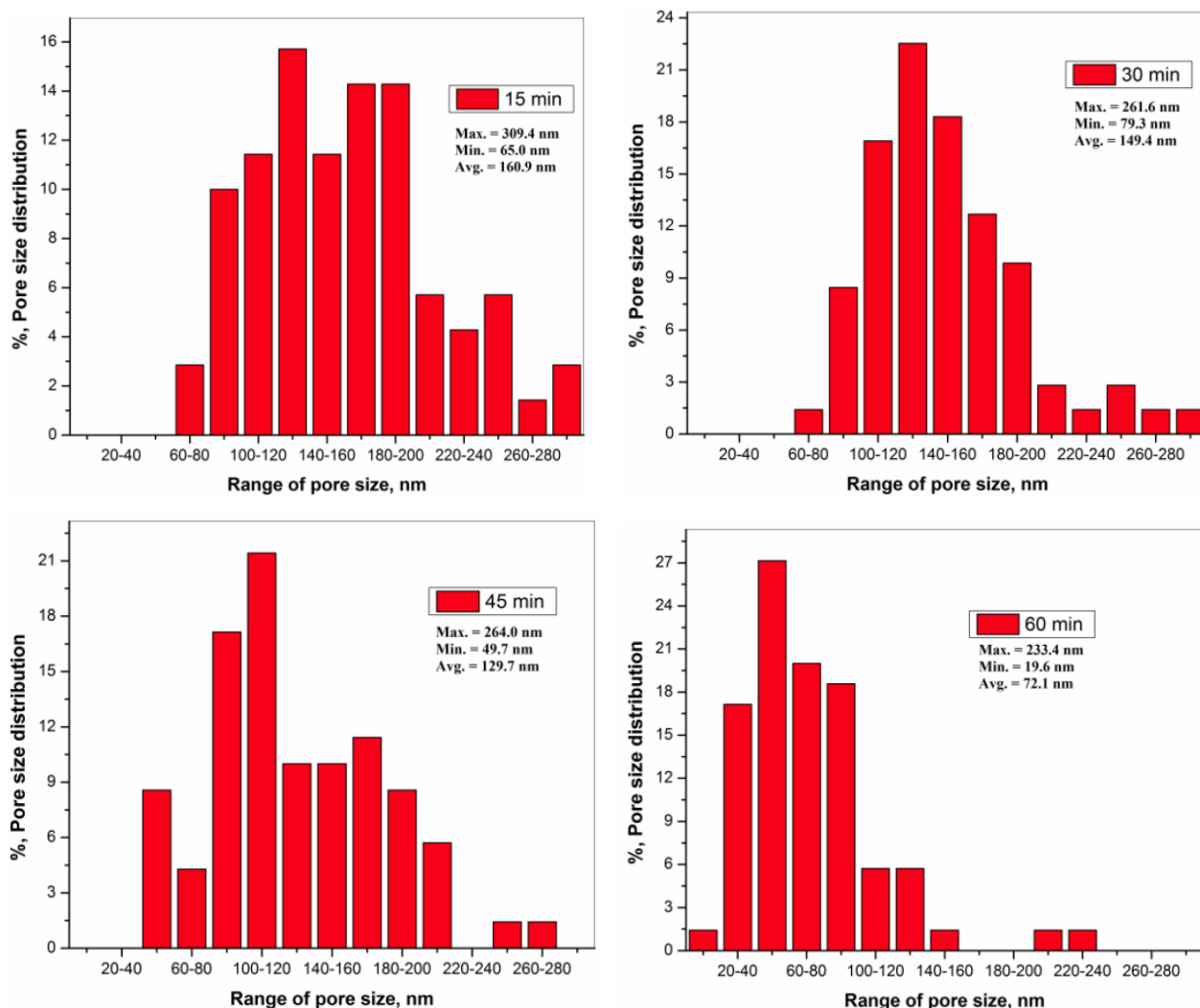


**Figure 9:** % Surface pore size diameter distribution of electro-spun PVA membranes obtained at different electro-spinning duration, 25 min, 35 min, 45 min and 60 min.

solution greatly and apply a larger stretching force within the solution causing in the fabrication of thinner fibers. Therefore, the effect of the electro-spinning duration alone on the fiber diameter distribution is not highly significant when compared with other parameters like, concentration and voltage supply. Due to this reason the distribution of fiber diameters of the four different samples deposited at 25, 35, 45, and 60 min indicated similar distribution. These results show a similar agreement with the statistical analysis of this study.

Electro-spinning method is an effective technique to produce nano meter range fibers and nanofibrous membranes with high porosity within nano to micrometer range pores [18]. The membrane surface pore size distribution was examined using image J software from the FESEM images. The pore size distributions are presented in Figure 9. As shown from

the results that the surface pore size of the electro-spun PVA membranes, increased as the electro-spinning duration time decreased. This result can be explained due to the fact that, increasing the electro-spinning duration means that we are allowing more fibers to be collected on the collector plate and the entanglements of the fibers were practically increased. In other words, more fiber layers were formed by increasing electro-spinning duration, where the surface pore was reduced due to the entanglements of the fibers layer-on-layer. Thus, the average surface pore diameters are measured as 72.1, 129.7, 149.4 and 160.9 nm for 60, 45, 35, and 25 min electro-spinning duration, respectively. Generally, all the membranes fall into ultrafiltration/microfiltration ranges. The decreasing of the average surface pore size is due to an increasing in the number of entangled fibers over and over as the electro-spinning duration increases from 25 to 60 min. Therefore, due to the increase in

entanglement of these fibers there is a possibility of formation of narrower net like structure which leads to the decrease of surface pore diameters of the membranes.

On the other hand, the thickness of the membranes has increased as the electro-spinning duration increases. The thickness measurement of the nanofiber membranes was performed using Lieca microscope as shown in Figure S1 in the Supplementary Information. The images revealed that the thickness of the membranes increased from 20 to 38  $\mu\text{m}$  for increasing electro-spinning duration from 25 to 60 min, respectively, in which the surface pore size is inversely proportional to membrane thickness [19]. But, the depth/flowing channel of the membrane pore is expected to increase with increasing thickness.

### 3.5. Cross-Linking of Electro-Spun PVA Membranes

The second objective of this work was to evaluate the effect of cross-linking on the properties of the membranes. When the electro-spun PVA membrane is immersed in water or used for water treatment applications, it can be dissolved slowly. In other words, the specific nanofibrous structures of electro-spun PVA membranes are not stable in aqueous condition. It is already well-known that polyvinyl alcohol can be cross-linked chemically with a range of aldehydes, like, glutaraldehyde and glyoxal [20]. The interaction is because of the development of acetal-bridges among the -OH within PVA and the aldehyde molecules [7, 21]. Crosslinking of electro-spun membrane was done at room temperature. Acetone, which is a water-miscible and a non-solvent for PVA, was mixed with hydrochloric acid (35 w %) and glutaraldehyde aqueous solutions (25 wt. %) in order to prepare the

crosslinking solution. The procedure of crosslinking solution preparation is clearly presented in Figure S4 (Supporting Information). No evidence of shrinkages was shown after the electro-spun PVA membrane was dipped into crosslinking solutions. The tested electro-spun PVA membranes were cross-linked by means of a mixture of acetone and 30 mM glutaraldehyde at 25  $^{\circ}\text{C}$  for 24 h [22]. Figure 10 shows the predicted chemical cross-linking reaction among the polyvinyl alcohol chains and glutaraldehyde catalysed using HCl [23]. The cross-linked electro-spun PVA membranes were rinsed numerous times and soaked in water for 48 hours and then dried.

#### 3.5.1. Infrared Spectroscopy (FTIR) Analysis

As shown in Figure 11, the interaction between PVA and GA catalysed by hydrochloric acid resulted in a substantial decrease in the intensity of the O-H peak, showing the development of acetal-bridges between the pendant hydroxyl groups of PVA chains [23]. Table 2 shows the typical band assignment of electro-spun PVA cross-linked with GA. As shown in Figure 11, the broad bands observed at  $3363\text{ cm}^{-1}$  are assigned to -OH stretching because of the presence of the strong bond (hydrogen bonding) of intra-molecular and inter-molecular type. The distinguishing bands at 1095, 1430 and  $2947\text{ cm}^{-1}$  were attributed to the C-O stretching, C-H bending and C-H stretching of PVA, respectively. The band observed at  $1714\text{ cm}^{-1}$  is may be due to the C=O stretching bands of remaining acetate group, residual after the synthesis of PVA during polyvinyl acetate hydrolysis process. The spectra show that there is no change in the molecular species and their interconnectivity when the process time is varied from 25 to 60 min.

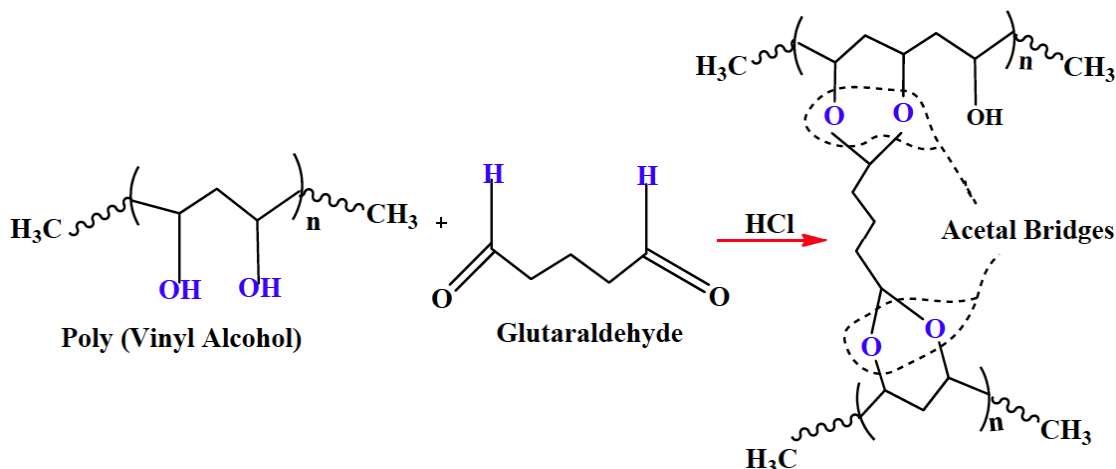


**Figure 10:** Schematic of cross-linked PVA formed by chemical reaction of PVA and glutaraldehyde catalysed by HCl.

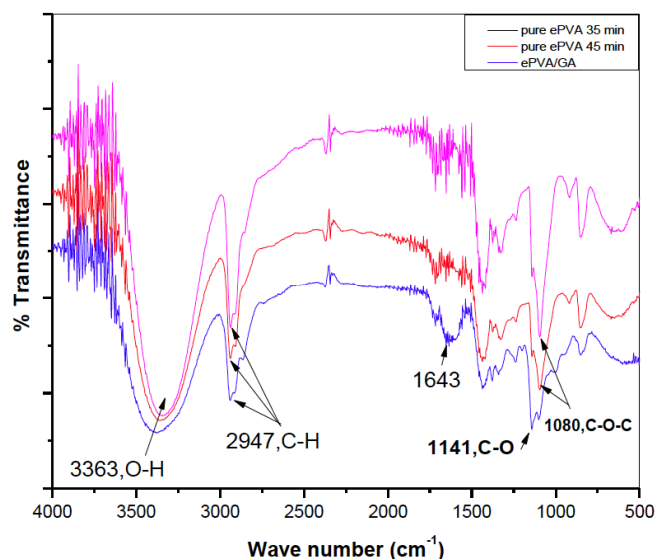


**Figure 11:** FTIR results of Electrospun PVA cross-linked with glutaraldehyde (ePVA/GA).

The presence of aldehyde peaks ( $\nu=1643\text{ cm}^{-1}$ ) could be because of the partial reaction of glutaraldehyde with the hydroxyl groups within the polyvinyl alcohol throughout the cross-linked network development. One aldehyde group could react with  $-\text{OH}$  groups within the polymeric chain by means of developing hemi-acetal structures due to its bi-functional cross-linker property. However, the other one does not interact which could be related with some kinetics drawbacks.

### 3.5.2. Thermogravimetric Analysis (TGA)

The thermogravimetric analysis (TGA) and differential thermogravimetry (DTG) curves for pure electro-spun PVA and PVA/GA membranes are presented in Figure 12a and b, respectively. The pure electro-spun PVA showed two main degradation steps at around  $220^\circ\text{C}$  and  $440^\circ\text{C}$  where the first stage was main degradation step and indicates the decomposition of side PVA chain [6]. The second smaller step was related to the splintering of the central chain of the pure electro-spun PVA membrane. The TGA curve for the electro-spun PVA/ GA membrane also indicated two

main degradation stages at around  $291^\circ\text{C}$  and  $480^\circ\text{C}$  and the first stage was main degradation step. It is clearly observed that the degradation temperatures of the electro-spun PVA/GA membranes are greater than that of pure electro-spun PVA membranes, which further indicates a rise in the thermal stability of the membrane after cross-linking process.

## 4. CONCLUSIONS

This study draws the conclusions of an empirical exploration using RSM method into the effects of time duration, voltage supply, concentration, and flow rate (while the distance and collector rotating speed were kept constant) on fiber diameter and surface pore size distribution during the preparation of electro-spun PVA membranes. Therefore, 10 wt. % aqueous PVA solutions were chosen as the optimized solution concentration; an applied voltage of 12 kV was selected throughout the process; and the feed rate was 1.0 mL/h by means of a 50 mL syringe using needle of 0.4 mm internal diameter. For further investigation on the effect of time duration, membranes were prepared at 25, 35, 45, and 60 min. Electro-spun PVA nanofiber membranes were successfully prepared at selected electro-spinning duration, cross-linked with glutaraldehyde and characterized. The average fiber diameters varied slightly between 88 to 124 nm when electro-spinning duration was varied. The surface pore size of the electro-spun PVA membranes, increased as the electro-spinning duration time decreased. Thus the average surface pore diameters are measured as 72.1, 129.7, 149.4, and 160.9 nm for 60, 45, 35, and 25 min electro-spinning duration, respectively. Generally, all the membranes fall into ultrafiltration/microfiltration ranges. In addition, no change in surface pore size and in fiber diameter after cross-linking was observed. However, crosslinking led to uniform arrangement of the fibers and increased network rigidity. The FESEM results agreed with the FTIR and TGA results in that the cross linker glutaraldehyde has reacted properly and confirmed the formation of an acetal-bridge. This

**Table 2:** Characteristic Bands of ePVA Crosslinked with GA and their Assignments

Range of Wavelength ( $\text{cm}^{-1}$ )	Assignment	Wave number, ( $\text{cm}^{-1}$ )	Reference
3000–2850	C–H stretch	2947	----
3500–3200	O–H stretch, H–bonded	3350	----
1670–1640	Carboxylic groups	1643	---
1150–1085	C–O–C	1080	[21]
1320–1000	C–O (Crystallinity)	1141	[23, 24]

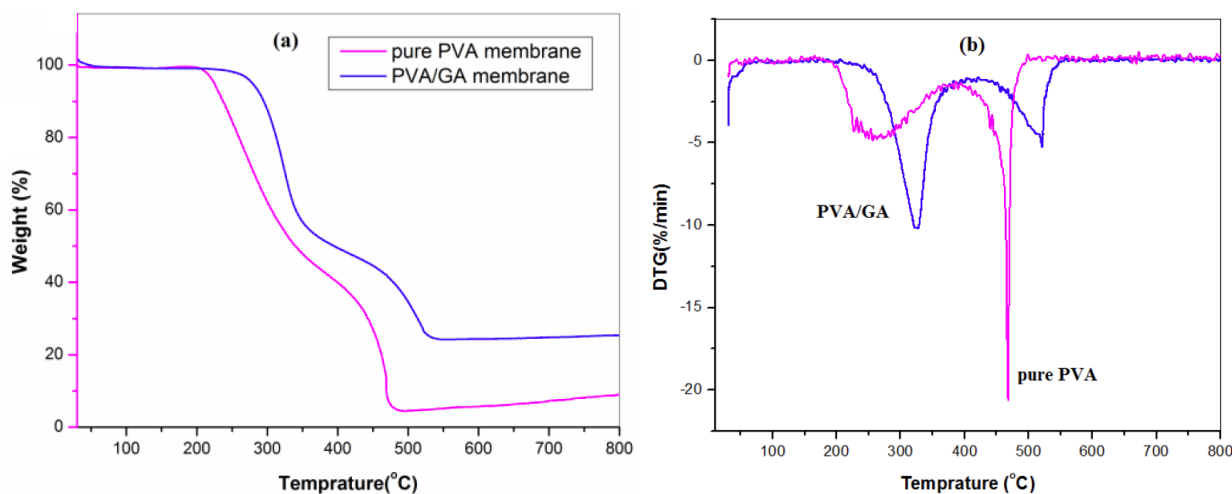


**Figure 12:** (a) TGA and (b) DTG curves of pure ePVA and ePVA/GA membranes.

study showed that the membrane properties can be controlled by varying the electro-spinning duration along with other process and solution parameters. Future studies will be needed to fully investigate the performance characteristics of the electro-spun PVA membranes for its flux, permeability and fouling performances.

## ACKNOWLEDGEMENTS

Central Instruments Facility (CIF), IIT Guwahati, India is thankfully acknowledged by the authors for allowing us to use FESEM and BET surface area and Prof. A. Srinivasan, Department of Physics, IIT Guwahati for allowing us the electro-spinning setup.

## SUPPORTING INFORMATION

The Supporting Information can be downloaded from the journal website along with the article.

## REFERENCES

- [1] Koski A, Yim K, Shivkumar S. Effect of molecular weight on fibrous PVA produced by electrospinning. *Mater Lett* 2004; 58(3-4): 493-497. [https://doi.org/10.1016/S0167-577X\(03\)00532-9](https://doi.org/10.1016/S0167-577X(03)00532-9)
- [2] Mohammad Ali Zadeh M, Keyanpour-Rad M, Ebadzadeh T. Effect of viscosity of polyvinyl alcohol solution on morphology of the electrospun mullite nanofibres. *Ceram Int* 2014; 40(4): 5461-5466. <https://doi.org/10.1016/j.ceramint.2013.10.132>
- [3] Xuefen Wang, Dufei Fang, Kyunghwan Yoon, Benjamin S. Hsiao, Chu B. High performance ultrafiltration composite membranes based on poly(vinyl alcohol) hydrogel coating on crosslinked nanofibrous poly(vinyl alcohol) scaffold. *J Membr Sci* 2006; 278(1-2): 261-268. <https://doi.org/10.1016/j.memsci.2005.11.009>
- [4] Yoon K, Hsiao BS, Chu B. High flux ultrafiltration nanofibrous membranes based on polyacrylonitrile electrospun scaffolds and crosslinked polyvinyl alcohol coating. *J Membr Sci* 2009; 338(1-2): 145-152. <https://doi.org/10.1016/j.memsci.2009.04.020>
- [5] Zhu X, Loo H-E, Bai R. A novel membrane showing both hydrophilic and oleophobic surface properties and its non-fouling performances for potential water treatment applications. *J Membr Sci* 2013; 436: 47-56. <https://doi.org/10.1016/j.memsci.2013.02.019>
- [6] Santos C, Silva CJ, Büttel Z, Guimarães R, Pereira SB, Tamagnini P, *et al.* Preparation and characterization of polysaccharides/PVA blend nanofibrous membranes by electrospinning method. *Carbohydr Polym* 2014; 99: 584-592. <https://doi.org/10.1016/j.carbpol.2013.09.008>
- [7] Yang Liu RW, Hongyang Ma, Benjamin S. Hsiao, Benjamin Chu. High-flux microfiltration filters based on electrospun polyvinylalcohol nanofibrous membranes. *Polymer* 2013; 54(2): 548-556. <https://doi.org/10.1016/j.polymer.2012.11.064>
- [8] Pugan JMC, Kim H-S, Lee K-J, Kim H. Low internal concentration polarization in forward osmosis membranes with hydrophilic crosslinked PVA nanofibers as porous support layer. *Desalination* 2014; 336: 24-31. <https://doi.org/10.1016/j.desal.2013.12.031>
- [9] Ramakrishna S, Fujihara K, Teo W-E, Lim T-C, Ma Z. *An Introduction to Electrospinning and Nanofibers* 1st edition ed, Singapore: World Scientific 2005. <https://doi.org/10.1142/5894>
- [10] Barhate RS, Loong CK, Ramakrishna S. Preparation and characterization of nanofibrous filtering media. *J Membr Sci* 2006; 283(1-2): 209-218. <https://doi.org/10.1016/j.memsci.2006.06.030>
- [11] Baş D, Boyacı İH. Modeling and optimization I: Usability of response surface methodology. *J Food Eng* 2007; 78(3): 836-845. <https://doi.org/10.1016/j.jfoodeng.2005.11.024>
- [12] Yördem OS, Papila M, Menceloğlu YZ. Effects of electrospinning parameters on polyacrylonitrile nanofiber diameter: An investigation by response surface methodology. *Mater Des* 2008; 29(1): 34-44. <https://doi.org/10.1016/j.matdes.2006.12.013>
- [13] Bezerra MA, Santelli RE, Oliveira EP, Villar LS, Escalera LA. Response surface methodology (RSM) as a tool for optimization in analytical chemistry. *Talanta* 2008; 76(5): 965-977. <https://doi.org/10.1016/j.talanta.2008.05.019>
- [14] Ferreira SLC, Bruns RE, da Silva EGP, dos Santos WNL, Quintella CM, David JM, *et al.* Statistical designs and response surface techniques for the optimization of chromatographic systems. *J Chrom A* 2007; 1158(1-2): 2-14. <https://doi.org/10.1016/j.chroma.2007.03.051>

- [15] Khanlou HM, Ang BC, Talebian S, Barzani MM, Silakhori M, Fauzi H. Multi-response analysis in the processing of poly (methyl methacrylate) nano-fibres membrane by electrospinning based on response surface methodology: Fibre diameter and bead formation. *Measurement* 2015; 65: 193-206.  
<https://doi.org/10.1016/j.measurement.2015.01.014>
- [16] Ahmadi pourroudosht M, Fallahiazouard E, Yusof NM, Idris A. Application of response surface methodology in optimization of electrospinning process to fabricate (ferrofluid/polyvinyl alcohol) magnetic nanofibers. *Mater Sci Eng C* 2015; 50: 234-241.  
<https://doi.org/10.1016/j.msec.2015.02.008>
- [17] Bose S, Das C. Role of Binder and Preparation Pressure in Tubular Ceramic Membrane Processing: Design and Optimization Study Using Response Surface Methodology (RSM). *Ind Eng Chem Res* 2014; 53(31): 12319-12329.  
<https://doi.org/10.1021/ie500792a>
- [18] Feng C, Khulbe KC, Matsuura T, Tabe S, Ismail AF. Preparation and characterization of electro-spun nanofiber membranes and their possible applications in water treatment. *Sep Purif Technol* 2013; 102: 118-135.  
<https://doi.org/10.1016/j.seppur.2012.09.037>
- [19] Ran Wang YL, Brandon Li, Benjamin S. Hsiao, Benjamin Chu. Electrospun nanofibrous membranes for high flux microfiltration. *J Membr Sci* 2012; 392-393: 167-174.  
<https://doi.org/10.1016/j.memsci.2011.12.019>
- [20] Yang E, Qin X, Wang S. Electrospun crosslinked polyvinyl alcohol membrane. *Mater Lett* 2008; 62(20): 3555-3557.  
<https://doi.org/10.1016/j.matlet.2008.03.049>
- [21] Zhang C-H, Yang F-I, Wang W-J, Chen B. Preparation and characterization of hydrophilic modification of polypropylene non-woven fabric by dip-coating PVA (polyvinyl alcohol). *Sep Purif Technol* 2008; 61(3): 276-286.  
<https://doi.org/10.1016/j.seppur.2007.10.019>
- [22] Xuefen wang, xuming chen, kyunghwan yoon, dufei fang, benjamin s. hsiao, chu b. High Flux Filtration Medium Based on Nanofibrous Substrate with Hydrophilic Nanocomposite Coating.pdf. *Environ Sci Technol* 2005; 39: 7684- 7691.  
<https://doi.org/10.1021/es050512j>
- [23] Mansur HS, Sadahira CM, Souza AN, Mansur AAP. FTIR spectroscopy characterization of poly (vinyl alcohol) hydrogel with different hydrolysis degree and chemically crosslinked with glutaraldehyde. *Mater Sci Eng C* 2008; 28(4): 539-548.  
<https://doi.org/10.1016/j.msec.2007.10.088>
- [24] Deepak AM, Ashwani K. Effects of surface crosslinking on sieving characteristics of chitosan: poly(acrylonitrile) composite nanofiltration membranes. *Sep Purif Technol* 2000; 21: 27-38.  
[https://doi.org/10.1016/S1383-5866\(00\)00188-X](https://doi.org/10.1016/S1383-5866(00)00188-X)

Received on 28-09-2016

Accepted on 19-12-2016

Published on 08-02-2017

DOI: <http://dx.doi.org/10.6000/1929-6037.2016.05.04.3>